Thermal radiation and chemical reaction effects with bioconvection of viscoelastic Walters' B liquid through porous medium–a numerical solution

Dyapa Hymavathi

Assistant Professor, Department of Mathematics, University College of Science,

Mahatma Gandhi University, Nalgonda, Telangana- 508254

Abstract: In this study, it is investigated how viscoelastic Walters'B fluid of swimming gyrotactic microorganisms (microbes) and solid nanoparticles transfer heat and mass over a horizontal porous substrate. Using appropriate boundary layer approximations, the flow model partial differential equations are replaced with conventional ones. The Keller Box method is used to numerically solve the dimensionless equations regulating the flow model as well as the boundary conditions, and the mass and heat flow characteristics are compared to the produced prime parameters that are taken into account for this issue. For resolving these differential equations with nonlinearity, the Keller Box method with the Matlab solver was used, and it was determined that this method is more accurate. Furthermore, parametric research concentrating on the influence of relevant parameters such as the local Nusselt number and local skin friction coefficient on velocity, temperature, salutal particle, and density of microorganisms is examined. It is discovered that the porous material significantly affects the problem's flow and thermal characteristics. The findings unmistakably demonstrate that a porous media increases skin friction and microbial motility density.

Keywords: Walter-B fluid, thermal radiation, chemical reaction, Gyrotactic microorganisms, horizontal porous medium.

Introduction:

MHD has been playing a very important role in the applications of fluid dynamics, biomedical engineering, in chemical engineering, medical sciences, and metallurgical sectors, and it is also used for both decontamination and filtration due to its extensive engineering and technological applications. It's crucial to research this class of fluids' flow issues. In many thermal systems, an improvement in heat transfer caused by nanofluids is necessary. Comparing nanofluids to conventional fluids, they have superior thermal conductivity. Different theories were used by different researchers to interpret the nanofluid flows. The focus of the scientific community has recently switched to the investigation of gyrotactic bacteria in nanofluid flows. In various bio microsystems, including nanochips, nanofluids containing microbes can be utilized to assess toxicity and optimize cellulose. The use of nanofluids including microorganisms in enzyme biosensors and microfluidic devices such as powdered micromixers and micro volumes is also advantageous.

The majority of the time, cooling is used to achieve the required end product features, and cooling speed is frequently managed by drawing the strips through a permeable medium. Non-Newtonian flow through a permeable medium has recently attracted a lot of attention. Fluid dynamics applications for boundary layer flow in saturated permeable media are numerous.

The categories into which non-Newtonian fluids are typically divided include Reiner-Rivlin fluids, Maxwell fluids, dilatant fluids, viscoplastic fluids, purely viscous fluids, \perfectly plastic materials, pseudo-plastic fluids, micropolar fluids, viscoelastic fluids, power-law fluids, Casson fluid, couple stress fluid, etc.

Currently, Walter's liquid model-B has been examined in this study. There are many different and varied uses for Walter's liquid model-B with mass and heat transmission, including those in the human body, vast petroleum industries, and daily living as well as in nature. Walter's liquid model-B has benefits over all the non-Newtonian fluid models. Unlike the viscoelastic fluid model, it is initially developed from the liquid's kinetic theory liquid instead of the experimental relation. Second, for fixed shear rates, it becomes Newtonian in nature. It's challenging technologically, but it's also challenging for engineers and applied mathematicians who demand accurate solutions.

The effect of Navier slip boundary conditions on steady-state radiative heat transfer flow of Walter's fluid B through a permeable medium is investigated by Mahabaleswara et al. [1]. Akinbo and Olajuwon [2] described the behavior of Walters' B liquid flow at the stagnation point with chemical reaction and radiation effects through a stretching sheet by imposing the Homotopy Analysis method. Chu et al. [3] studied Pressure and buoyancy forces on Walter' B fluid through a stretching sheet incorporated joule heating and chemical reaction under the deposition of thermophoresis particles. Rajkumar et al. [4] analyzed the Hall and Ion slip conditions over an abruptly infinite vertical plate over a permeable medium with the influences of Dufour effect and thermal radiation MHD unsteady Walter's B fluid model. A viscoelastic flow of fluid model was created by Sajid et al. [5] over a lubricated surface at a stagnation point. In their research, Tonekaboni et al. [6] created a non-newtonian fluid model called Walter's B fluid model for boundary layer flows as Sakiadis flows, Blasius flows, and stagnation point flows.

An effect of variable viscosity on MHD dusty Walter's fluid B modeling a porous medium is investigated by Prakash et al. [7], Using the scientific computing program Mathematica, Singh et al. [8] discussed the effects of varying wall temperature and ions slip conditions on the intermittent flow through the boundary layer of rotating Walter's B liquid over uniform porous media. Mahat et al. [9] focused on the analysis of the impact of mixed convection and radiation on Walter's Bliquid model flow via a circular cylinder under convective boundary conditions and constant heat flux horizontally by imposing of Keller Box method. Ghani et al. [10] Created Walter's fluid B model that describes how a horizontal permeable plate flows under the impact of a convective magnetic field. Between two juxtaposed horizontal flat plates loaded with a nanofluid including both nanoparticles and gyrotactic microorganisms, Xu et al. [11] explored the fully formed mixed convection flow and the effect of nanoparticles on bio convection. For the development of the energy equation, a novel slip mechanism non-linear combined bioconvective flow over a stretching surface is considered, and subject to

chemical reaction mass transfer rate is discussed by Khan et al. [12]. At the stretched boundary of the sheet, Chu et al. [13] studied the flow behavior of heat and solutes stratification effects, and the total residual error was determined using the Homotopy analysis approach. Impact of inclined magnetic field viscous dissipation and stratification flow of Walter B nanofluid past a horizontal cylindrical surface identified by Naz et al. [14] In the presents of Arrhenius activation energy, velocity slip, and radiation rheology of 3-D Eyring- Powel nanofluid is explored by Khan et al. [15]. Hayat et al. [16] examined the density of gyrotactic microbes and melting events in the context of thermal diffusion and diffusion-thermo effects on bioconvection Walter-B nanofluid flow. More recently the authors have investigated the behavior of bioconvection of nanofluids with the swimming of gyrotactic microorganisms under various impacts and geometrical conditions [17-19]. Oke et al. [20] examined the impact of thermal radiation and Coriolis force on hybrid nanofluid flow through an exponentially stretching plate. Shi et al. [21] analyzed the bio-convection magneto-cross nanofluid flow with the energy of activation including gyrotactic microorganisms. Gowda et al. [22] examined the mass and heat transfer of non-Newtonian nanofluid with activation energy and binary chemical reaction. Kumar et al. [23] scrutinized the effect of thermal diffusion and diffusion-thermo on the Walters-B fluid flow through a sheet embedded in a permeable media.

In contrast to Newtonian fluids, viscoelastic fluids' constitutive equations frequently result in higher-order derivative factors in the acceleration equations. The focus of the current contribution is, above all, on investigating the impact of mass and heat transfer on the flow of magneto-Walter's B nanofluid with the impact of thermophoretic applications, buoyant forces, and nonlinear thermal radiation. Since the effects of thermal radiation are thought to be nonlinear, the problem is quite adaptable. The viscoelastic effects are present in the non-Newtonian Walter's B fluid. The viscoelastic Walters' B boundary layer flow difficulties are solved similarly in this study, and all of the equations are reduced into nondimensional forms. These nonlinear differential equations are solved using the given fourth-order equations, and accurate results are obtained. This approach is found to be easier to use and more accurate.

Our research might also improve the efficiency of microbial fuel cells. Gyrotactic bacteria can also make nanofluids in a flow more stable. As nutrient, organisms are injected into the oil transporting layer, a microbially enhanced oil restoration frequently uses bioconvection mechanisms to sustain the shift in permeability.

Mathematical formulation:

The fact that the bacteria can only exist in water is important to note. This suggests that water must be the base fluid to be taken into account. On the contrary hand, it is considered that the nanoparticles dispersed in the base fluid are stable and do not group. Additionally, it is expected that the bacteria' swimming direction and speed are unaffected by the nanoparticles. Additionally, the nanofluid employed in this study needs to be diluted to prevent bioconvection instability brought on by an increase in the viscosity of the suspension. Using these

presumptions and the nanofluid model put forward by Kuznetsov and Nield [24], the following five field equations are provided. These equations represent the conservation of total mass, momentum, thermal energy, nanoparticle volume fraction, and microorganisms.

$$\nabla.V = 0, \quad (1)$$

$$\rho_f(V.\nabla).V = -\nabla p + \mu\nabla^2 V, \quad (2)$$

$$V.\nabla T = \alpha\nabla^2 T + \tau\left[D_B\nabla T.\nabla C + \left(\frac{D_T}{T_\infty}\right)\nabla T.\nabla T\right], \quad (3)$$

$$(V.\nabla)C = D_B\nabla^2 C + \left({}^{D_T}/_{T_0}\right)\nabla^2 T, \quad (4)$$

$$\nabla.j = 0, \quad (5)$$

Here, V represents the nanofluid flow's velocity and $V = (u, v)$ with the u and v velocity components located in the x- and y-directions, respectively.C is the nano particle volumetric fraction, ρ_f is the nanofluid density, T is temperature,p is pressure, $\mu$is the suspension's viscosity of microorganisms and nanofluid, $\alpha$is the nanofluid's thermal diffusivity, a parameter with the formula $\tau = {(\rho c)_p}/{(\rho c)_f}$ has $(\rho c)_p$ as the heat capacity of the nanoparticle and $(\rho c)_f$ as the heat capacity of the fluid,T_0 is a reference temperature, the coefficient of thermophoretic diffusion is D_T, D_B is the Brownian diffusion coefficient.

According to the definition given by, J is the flux of microorganisms brought about by fluid convection, and diffusion, self-propelled swimming

$J = NV + N\hat{V} - D_n\nabla N$in which, $\hat{V} = \left({}^{bW_c}/_{\Delta C}\right)\nabla C$ is the velocity vector relating to the cell swimming in nanofluids with D_n being the microorganisms diffusivity, W_c being the maximum cell swimming speed $[m/s]$, b being the chemotaxis constant $[m]$, and the motile density of microorganisms is N,

In order to solve this problem, a steady two-dimensional flow with constant velocity $U_w$and free stream velocity $U_\infty$was assumed. The x-axis and y-axis were both parallel to the plate. The momentum equation employs Walters' B fluid as the tensor type Ref. 6 and Ref 7. The following updated mathematical model, investigated in [25], is built using Newton's second law, the law of conservation of mass, and the law of thermodynamic energy.

$$\frac{\partial u}{\partial x} + \frac{\partial u}{\partial y} = 0, \quad (6)$$

$$u\frac{\partial u}{\partial x} + v\frac{\partial u}{\partial y} = \frac{\mu_0}{\rho}\left(\frac{\partial^2 u}{\partial y^2}\right) - \frac{k_0}{\rho}\left(u\frac{\partial^3 u}{\partial x\partial y^2} + v\frac{\partial^3 u}{\partial y^3} - \frac{\partial u}{\partial y}\frac{\partial^2 u}{\partial x\partial y}\right) - \frac{k_0}{\rho}\left(\frac{\partial u}{\partial x}\frac{\partial^2 u}{\partial y^2}\right) - \frac{1}{\rho}\sigma u B_0^2 - \frac{\nu}{k}u$$

(7)

$$u\frac{\partial T}{\partial x} + v\frac{\partial T}{\partial y} = \alpha\frac{\partial^2 T}{\partial y^2} + \frac{\nu}{c_p}\left(\frac{\partial u}{\partial y}\right)^2 + \tau\left[D_B\frac{\partial C}{\partial y}\frac{\partial T}{\partial y} + \frac{D_T}{T_\infty}\left(\frac{\partial T}{\partial y}\right)^2\right] - \frac{1}{(\rho c_p)_f}\frac{\partial q_0}{\partial y} + \frac{Q_0}{(\rho c_p)_f}(T - T_\infty)$$

(8)

$$u\frac{\partial C}{\partial x} + v\frac{\partial C}{\partial y} = D_B\frac{\partial^2 C}{\partial y^2} + \frac{D_T}{T_\infty}\frac{\partial^2 T}{\partial y^2} - kr(C - C_\infty) \quad (9)$$

$$u\frac{\partial N}{\partial x}+v\frac{\partial N}{\partial y}=D_n\frac{\partial^2 N}{\partial y^2}-\frac{1}{(C_w-C_\infty)}\left(N\frac{\partial^2 C}{\partial y^2}\right)bW_c+D_n\frac{\partial^2 N}{\partial y^2} \quad (10)$$

With boundary conditions

$$u=U_x,\ v=V_x,\qquad T=T_w,\qquad C=C_w,\qquad N=N_w\ \ at\ y=0$$

$$u=U_\infty,\frac{\partial u}{\partial y}=0,\ T=T_\infty,\ C=C_\infty,\ N=N_\infty,\ as\ \ y\to\infty \quad (11)$$

Ψ is stream function to analyze the boundary layer for velocity and temperature. And the velocity components are as follows $u=\frac{\partial \Psi}{\partial y},\ and\ \ v=-\frac{\partial \Psi}{\partial x}$which can be transformed by consider

$$\Psi=\sqrt{2U_\infty x\nu}f(\eta),\ \eta=\sqrt{\frac{U_\infty}{2x\nu}}y,\quad \theta(\eta)=\frac{T-T_\infty}{T_w-T_\infty},$$

$$\phi=\frac{C-C_\infty}{C_w-C_\infty},\ \ g(\eta)=\frac{N-N_\infty}{N_w-N_\infty} \quad (12)$$

By substituting the above considerations in the governing equations (6) - (10) and boundary conditions can be obtained as

$$f'''+ff''+\frac{K}{2}(ff''''+f'f'''-(f'')^2)-Mf'-Kf'=0, \quad (13)$$

$$\left(\frac{1}{Pr}+\frac{4}{3}R\right)\theta''+f\theta'+Nb\theta'\phi'+Nt(\theta')^2+Ec(f'')^2+Q\theta=0, \quad (14)$$

$$\frac{1}{Sc}\phi''+f\phi'+\frac{Nt}{Nb}\theta''-A\phi=0, \quad (15)$$

$$\frac{1}{Sb}g''+fg'-Pe(g'\phi'+(\Omega+g)\phi'')=0, \quad (16)$$

With the associated boundary conditions

$$f(0)=f_w,\qquad f'(0)=\lambda_m,\ \theta(0)=1,\qquad g(0)=1,\phi(0)=1$$

$$f'(\infty)=1,\ f''(\infty)=0,\ \theta(\infty)=0,\ \phi(\infty)=0,\ g(\infty)=1, \quad (17)$$

Where the non dimensional parameter

$$K=\frac{k_0U_\infty}{\rho\nu}\ ,\ M=\frac{k_0U_\infty}{\rho\nu},\ K=\frac{\nu}{k}\sqrt{\frac{k_0}{g\beta T_w}},\ Pr=\frac{\alpha}{\nu},\ R=\frac{4\sigma^*T_\infty^3}{\nu k^*(\rho c_p)},\ Nb=\frac{\tau D_B(C_w-C_\infty)}{\nu},\ Nt=\frac{D_T}{T_\infty\nu}(T_w-T_\infty),$$

$$Ec=\frac{U_\infty^2}{c_p(T_w-T_\infty)},Q=\frac{2xQ_0}{(\rho c_p)U_\infty},\ Sc=\frac{D_B}{\nu},A=\frac{2xk}{U_\infty},\ Sb=\frac{D_n}{\nu}\ ,Pe=\frac{bw_c}{\nu}\ ,\Omega=\frac{N_\infty}{(N_w-N_\infty)},\ \lambda_m=\frac{U_w}{U_\infty}$$

Methodology:

The Keller-box method is used to solve the given boundary layer system of ordinary differential equations (13)-(16), and it is well known method of implicit finite difference for accuracy. It is second order accuracy method. Equations (13) –(16) with boundary conditions (17) are transformed using this technology into initially first order equations by assuming the following

$$f'=p,\ p'=q,f'=p,\ \theta=s,q'=r,\ \ s'=t,\ \phi=h,\ h'=n,\ g'=u$$

further by finite difference approximations the obtained first order equations are converted into nonlinear equations and those nonlinear equations are linearised by imposing by Newton's method later with LU

decomposition method the obtained matrix of order 10X10 is solved with Matlab solver, the results are represented through graphs and analyzed for various parameter's nature. After many trials the convergence stage is tested, the accuracy is fixed at $10^{-6}$and $\nabla\eta = 0.001$

Results and Discussions:

The set of linked fourth order ordinary differential equations has been solved, including the boundary conditions numerically by using Keller- box mechanism through with skin friction, Nusselt number Sherwood number, concentration, temperature, the velocity of nanofluids also density of the motile microorganisms is analyzed. For affixed values of $K = 2.0;\ P = 0.2;\ Pr = 0.7;\ R = 0.8;\ Ec = 0.2;\ Q = 0.0;\ Nb = 0.3; Sc = 0.6;\ Nt = 0.6;\ A = 1.0;\ Sb = 1.2;\ \Omega = 0.1;\ Pe = 0.2;\ M = 2.0;$

The numerical values of $-f''(0), -\theta'(0), -\phi'(0), -g'(0)$ for various parameters and the nature of other physical quantities are also observed in the table1, table 2, and table 3.

Table 1 shows that raising the magnetic field parameter M and Eckert number decreases the rate of heat transfer while increasing the skin friction coefficient, Sherwood number, and motile rate of microorganisms improves flow behavior. **Table 1:**

R	M	Ec	Pr	$-f''(0)$	$-\theta'(0)$	$-\phi'(0)$	$-g'(0)$
0.1				0.121849	0.327538	0.279637	0.241683
0.2				0.126105	0.329530	0.280362	0.242301
0.3				0.130335	0.331407	0.281088	0.242908
0.4				0.134538	0.333175	0.281818	0.243505
	0.1			0.108835	0.329230	0.276912	0.240302
	0.2			0.112294	0.328801	0.277662	0.240686
	0.3			0.115606	0.328376	0.278363	0.241043
	0.4			0.118787	0.327955	0.279019	0.241374
		0.1		0.121849	0.327538	0.279637	0.241683
		0.2		0.121947	0.292139	0.286590	0.242066
		0.3		0.122045	0.256693	0.293551	0.242449
		0.4		0.122143	0.221201	0.300521	0.242832
			0.71	0.121849	0.327538	0.279637	0.241683
			1	0.121547	0.357319	0.274185	0.241373
			2	0.120951	0.415350	0.263694	0.240773
			3	0.120649	0.443305	0.258693	0.240486

Table 2 shows how Brownian motion and thermophoresis affect the flow transfer rate of microorganisms swimming. Microorganisms' Nusselt number, Sherwood number, and motile rate in nanofluids are improved.

Table 2

Nb	Nt	$-f''(0)$	$-\theta'(0)$	$-\phi'(0)$	$-g'(0)$
0.1		0.095203	0.313478	0.216509	0.228738
0.2		0.095203	0.302805	0.222543	0.228784
0.3		0.095203	0.292307	0.224549	0.228799
0.4		0.095203	0.281987	0.225547	0.228807
	0.1	0.095203	0.324618	0.216509	0.228738
	0.2	0.095203	0.313613	0.222543	0.228784
	0.3	0.095203	0.308218	0.224549	0.228799
	0.4	0.095203	0.279816	0.225547	0.228807

Table 3 shows that Peclet number Pe, a bioconvection parameter, increases the flow rate of Skin friction, Nusselt number, Sherwood number, and microorganism motility, whereas Schmidt number Sc decreases the rate of thermal transfer while increasing the flow rate of Skin friction, Sherwood number, and microbe motility. The chemical reaction parameter, on the other hand, enhances the flow transfer rate of skin friction and heat transfer, as measured by the Nusselt number, but reduces the nanoparticle transfer rate and the motile rate of microorganisms.

Table 3

Pe	Sb	Sc	A	$-f''(0)$	$-\theta'(0)$	$-\phi'(0)$	$-g'(0)$
1				0.121852	0.327542	0.279639	0.250762
2				0.121859	0.327549	0.279642	0.269255
3				0.121866	0.327556	0.279645	0.288189
4				0.121873	0.327563	0.279648	0.307556
	0			0.121989	0.327683	0.279697	0.576355
	2			0.122064	0.327741	0.279721	0.855122
	4			0.122110	0.327770	0.279732	0.855122

	8			0.122143	0.327789	0.279739	1.318256
		0.1		0.121829	0.328161	0.240942	0.239920
		0.2		0.121849	0.327538	0.279637	0.241683
		0.3		0.121866	0.326995	0.316063	0.243368
		0.4		0.121881	0.326524	0.350326	0.244974
			0.1	0.121849	0.327538	0.279637	0.241683
			0.2	0.124766	0.327659	0.279414	0.241568
			0.3	0.127640	0.327774	0.279205	0.241460
			0.4	0.130471	0.327883	0.279008	0.241359

The results are analyzed graphically. The profile for different values of the magnetic field parameter M is shown in Figures 1(a)–1(d).The observation is that the velocity profile initially increases after at the rate of convergence of the momentum, as the magnetic field strength increases throughout the fluid region, the velocity profile slowly decreases. A force known as the Lorentz force is created when a magnetic field is applied to an electrically conducting fluid. This results in a decrease in fluid velocity within the boundary layer, which opposes the transport phenomenon, while the temperature and microbe density rise, and the concentration of nanoparticles have a decreased volume fraction profile.

Porosity is the ratio of pore volume to its total volume. Because of these nature figures 2(a) - 2(d) shows with rises in porous parameters, the momentum profile increases and after an amount of time the velocity is decreasing whereas the temperature and density of motile microorganisms is increasing while the concentration profile of nanoparticle is decreasing. Prandtl number Pr denotes the relation between momentum diffusivity and thermal diffusivity. Lower Prandtl number Pr, results in higher thermal diffusivity the gradual thinning of the boundary layer characterizes shear thickening activity. According to the definition, as a result of 3 (a)-3(c) of the thermal profile, Pr is inversely related to thermal diffusivity and the concentration of nanoparticles profile increases whereas the density of microorganism is decreasing. The Brownian motion parameter influences heat transfer. Heat transfer enhancement varies from particle to particle due to differences in Brownian motion effects.

According to figures 4(a)–4(c), the temperature and the density of microorganisms are falling, while the concentration of the volume fraction profile of nanoparticles is rising. When small particles are pulled from a hot surface to a cold one, a process known as thermophoresis occurs. As a result, a hot surface loses a lot of its small particles, which raises the temperature. Figures 5(a)-5(c) can be represented that thermal boundary layer enhances, and mass diffusion boundary layer of nanoparticle is increasing and at point of time decreasing

gradually. As the thermophoresis parameter increases, the density of motile microorganisms decreases. As a result, 6(a)-6(c) the productive chemical reaction A causes the up rises in thermal boundary layer, mass diffusion layer, and density of motile microorganisms. Schmidt number Sc influences the convection and characterizes liquid flows. It is described as the relationship between momentum and mass diffusivity. Physical terms include the mass transport layer and the hydrodynamic thickness layer. The smaller Schmidt number Sc is correlated with increased nanoparticle concentration. Based on graphical interface 7(a)-7(c), temperature profile and concentration profiles are decreasing while the density of motile microorganisms increases.

Peclet number Pe values that are higher indicate that microorganisms diffuse more slowly, therefore, loss of motile density of nanoparticles is examined with this behavior, from the figure 8, while Peclet number Pe increases the density of motile microorganisms is decreased. An expanding number of bioconvection parameters Sb the velocity, and temperature profiles are increasing as well as a decline in the density of mobile microorganisms while concentration of nanoparticle profile is initially decreasing and then it is increasing seen in the figure 9 (a)- 9 (d). The thermal boundary layer profile is increased by higher values of the radiation parameter R R because more heat is transferred to the working fluid via radiation phenomena. Hence thermal boundary layer thickness becomes increase in th radiation parameter upsurges the thermal distribution phenomenon as a result 10 (a)- 10(c) temperature escalates also the concentration of nanoparticle prof is upsurges while the density of motile microorganism is decreases. Figures 11(a)–11(c) demonstrate that the thermal boundary layer profile and the mass per unit area of motile microorganisms both increase with an upsurge in Eckert number, but the concentration of nanoparticle volume fraction profile drops. From tigures12 (a) – 12(c) similar behaviors can be observed in the case of thermal generation and absorption. Internal heat generation/ absorption either improves or dampers the heat transfer. The larger heat generation/ absorption enhances the thermal profile to put it mechanically, an upsurge in heat source intensity leads to a larger thermal diffusion layer, which may lead to an upsurge in the diffusion of the temperature gradient. As a result, while the nanoparticle volume fraction concentration profile is falling, the thermal profile and motile microorganisms' density are augmenting.

Graphical results 1(a)-1(d) represent the impacts of magnetic parameter M on temperature, velocity, nanoparticle concentration, and motile microorganism density profiles

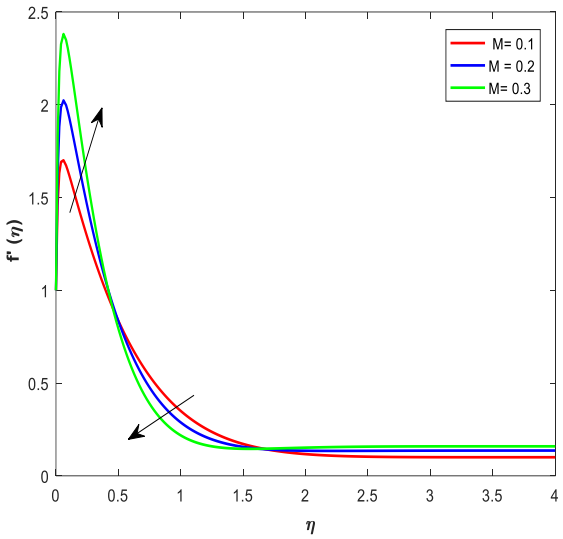

Result 1 (a)

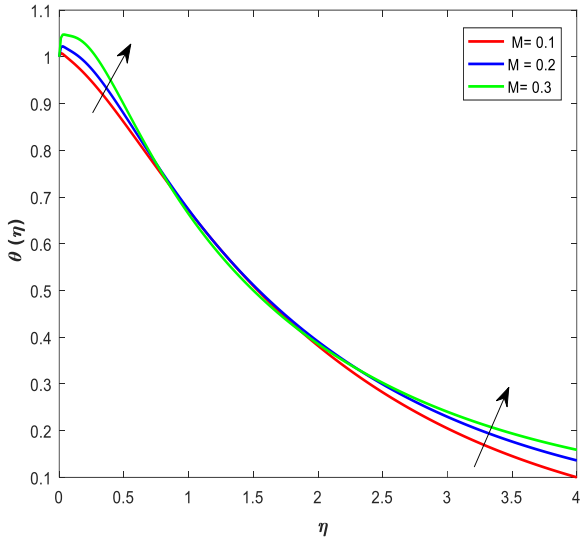

Result 1(b)

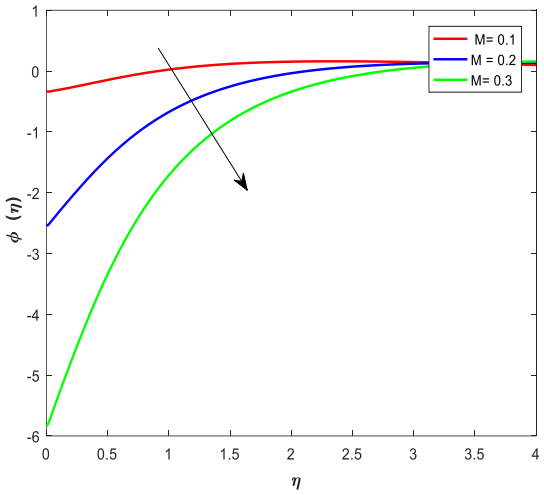

Result 1(c)

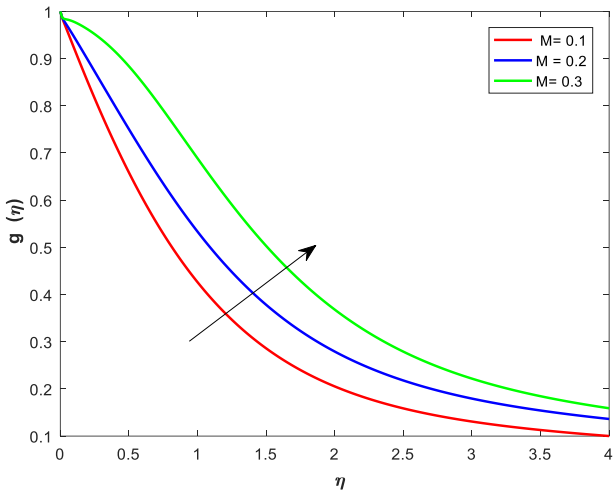

Result 1(d)

Graphical results 2(a)-2(d) represent the impacts of porous media parameter P on molecular motility, temperature, nanoparticle concentration, and density profiles

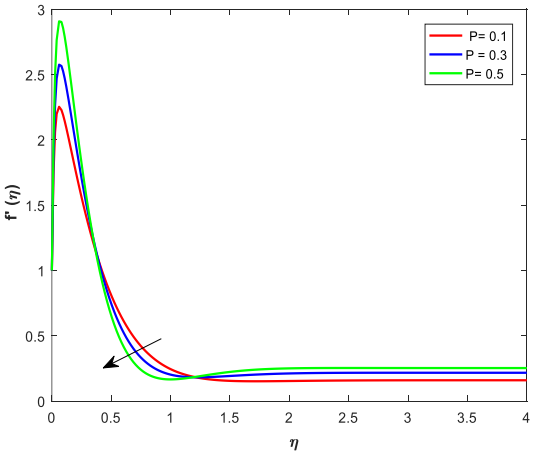

Result 2(a)

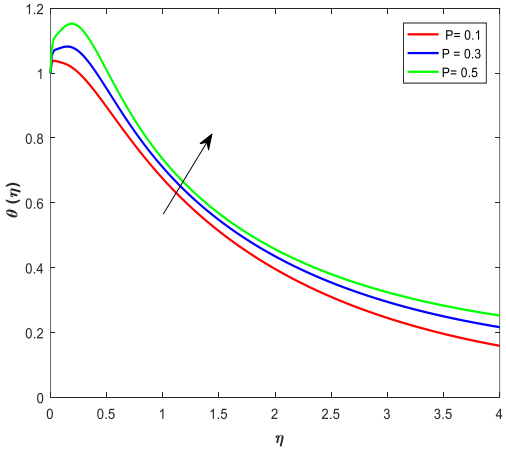

Result 2(b)

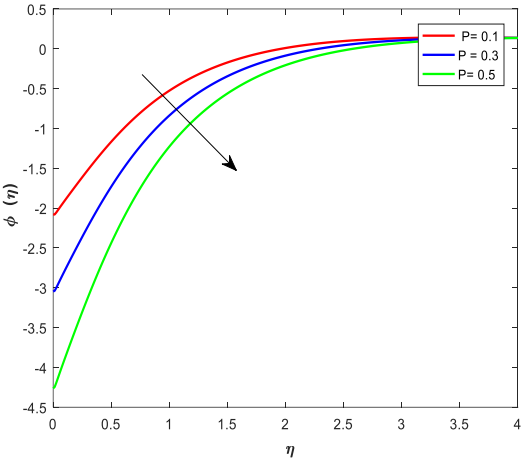

Result 2(c)

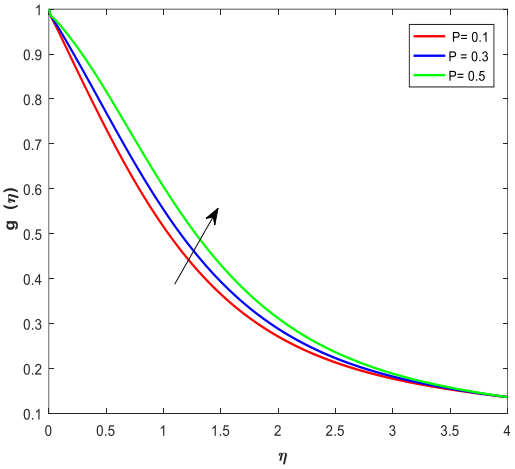

Result 2(d)

Graphical results 3(a)-3(c) represent the impacts of Prandtl number Pr on concentration, temperature, nanoparticles, and density of motile microorganisms' profiles.

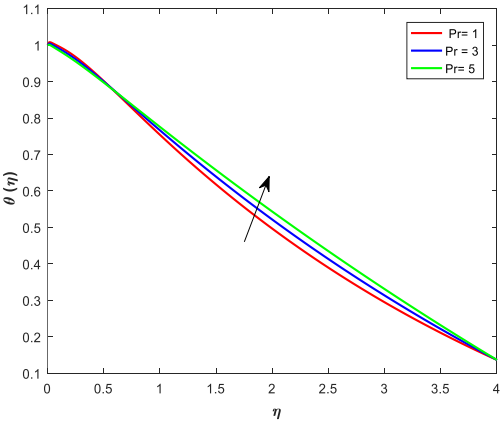

Result 3 (a)

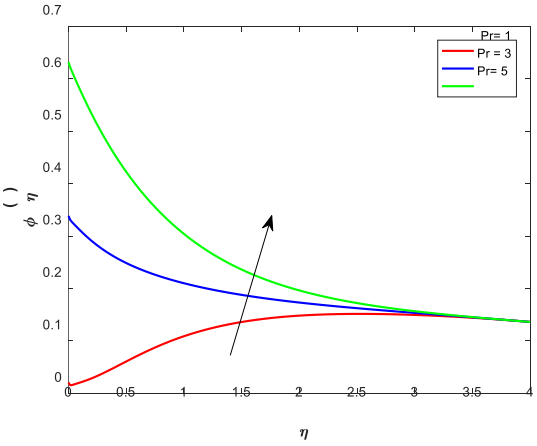

Result 3(b)

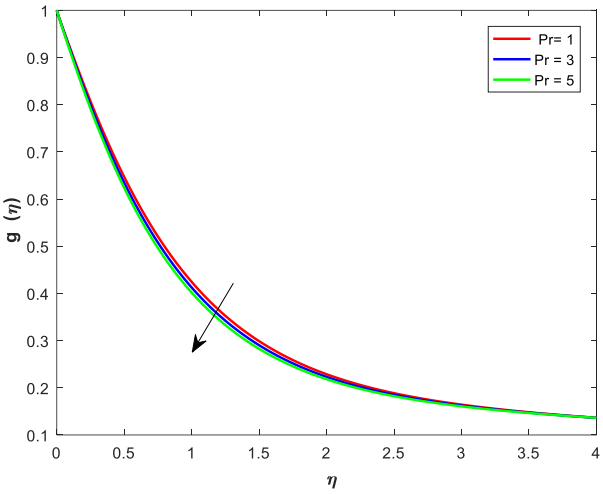

Result 3(c)

Graphical results 4(a)-4(c) represents the impacts of Brownian motion parameter on temperature, the concentration of nanoparticle, and the density of motile microorganism profiles

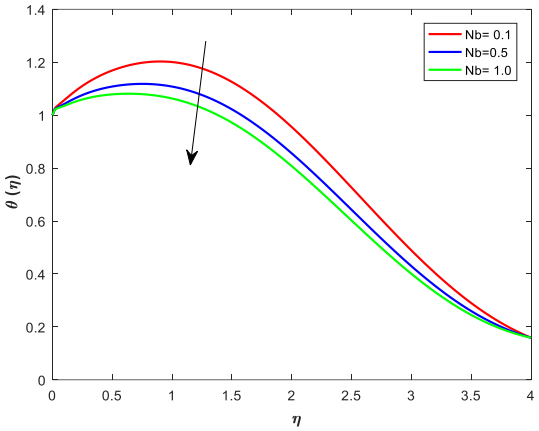

Result 4 (a)

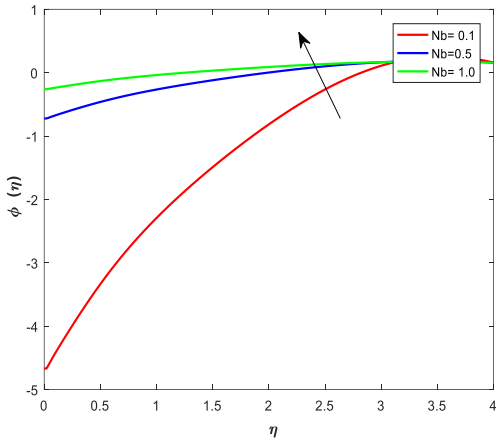

Result 4(b)

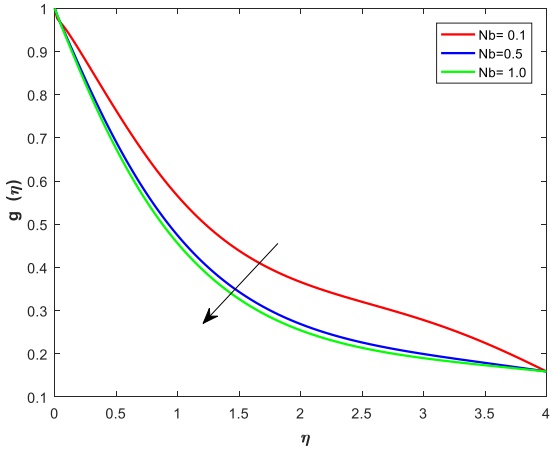

Result 4(c)

Graphical results 5(a)-5(d) represents the impacts of thermophoresis parameter on temperature, the concentration of nanoparticle, and the density of motile microorganisms' profiles

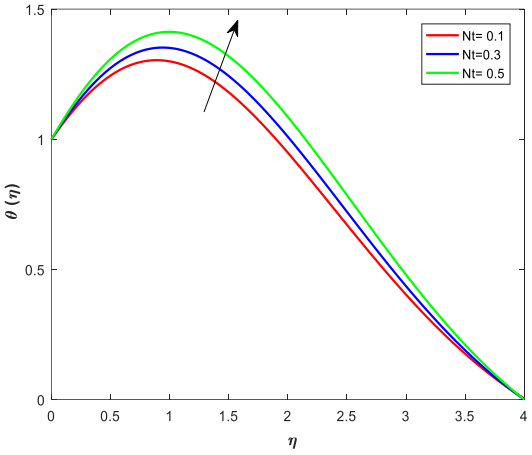

Result 5(a)

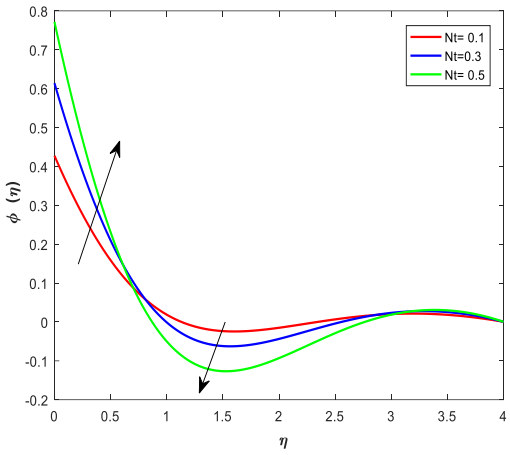

Result 5(b)

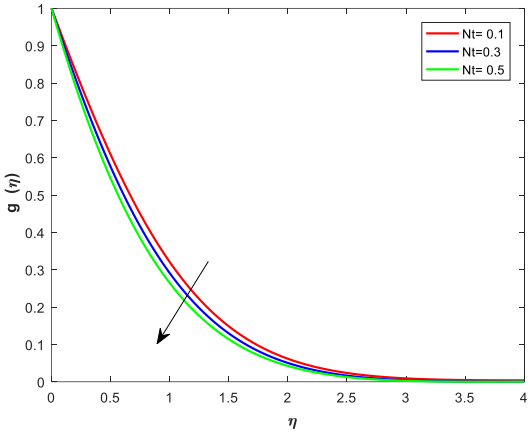

Result 5(c)

Graphical results 5(a)-5(d) represents the impacts of chemical reaction parameter on temperature, the concentration of nanoparticle, and the density of motile microorganisms' profiles

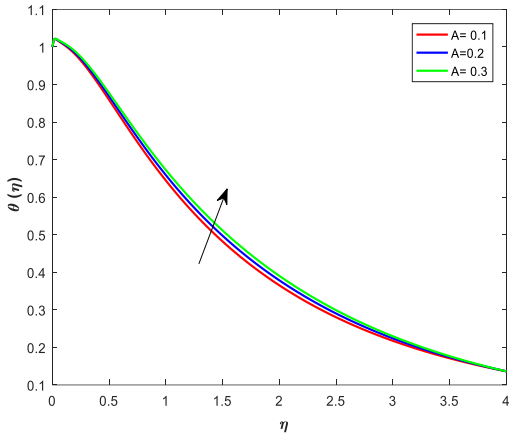

Result 6(a)

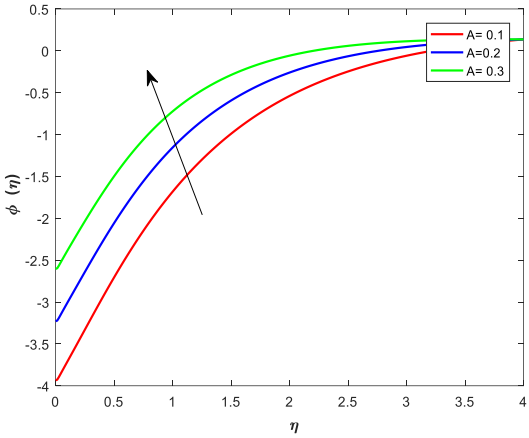

Result 6(b)

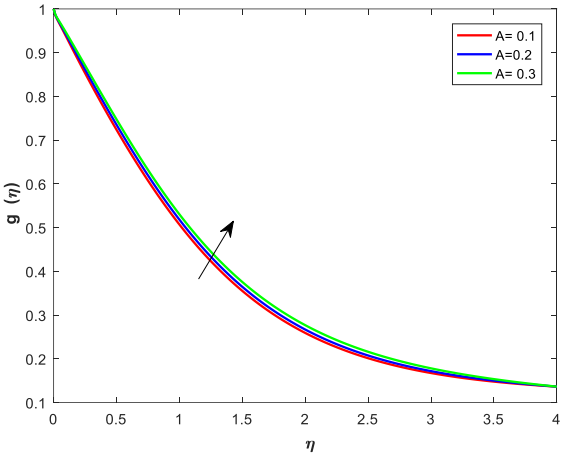

Result 6(c)

Graphical results 7(a)-7(d) represents the impacts of the Schmidt number on temperature, the concentration of nanoparticle, and the density of motile microorganisms' profiles

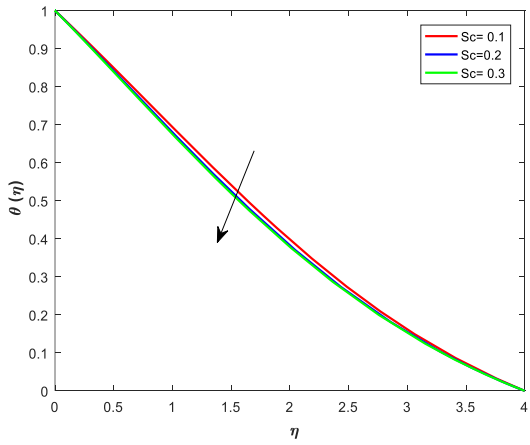

Result 7(a)

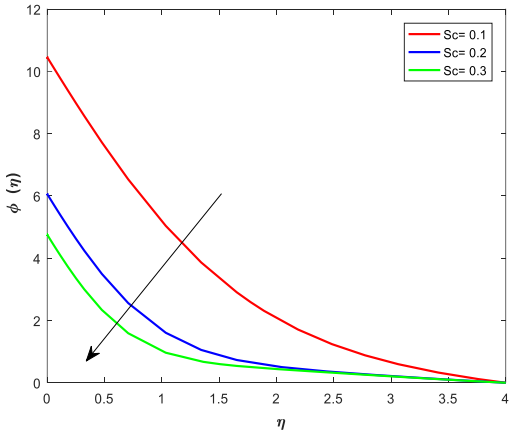

Result 7(b)

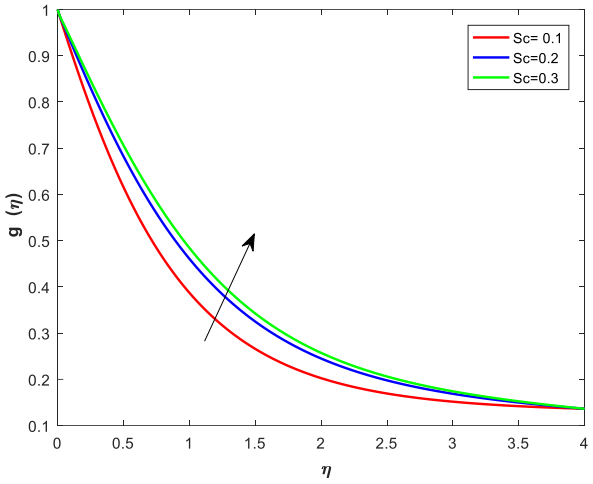

Result 7(c)

Graphical results 8 represents the impacts of Peclet number on the density of motile microorganisms profiles

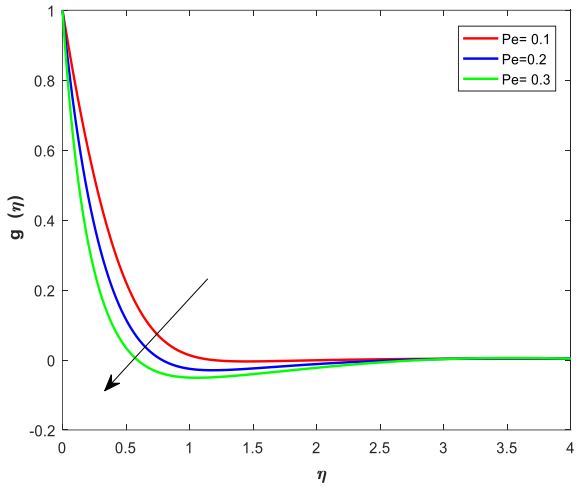

Result 8

Graphical results 9(a)-9(d) represent the impacts of Sb number on momentum, temperature, the concentration of nanoparticles, and density of motile microorganisms' profiles

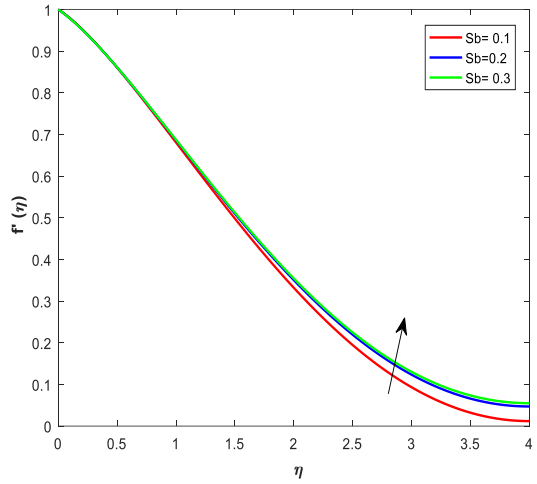

Result 9(a)

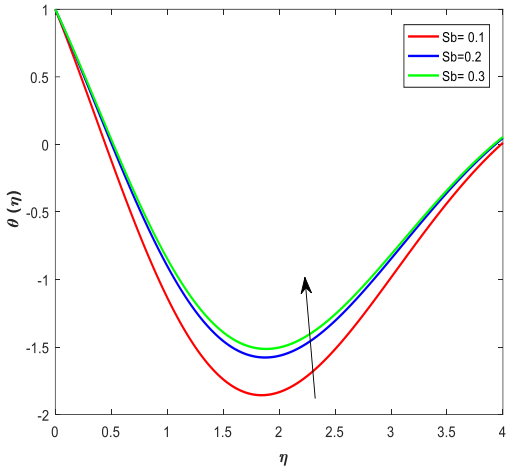

Result 9(b)

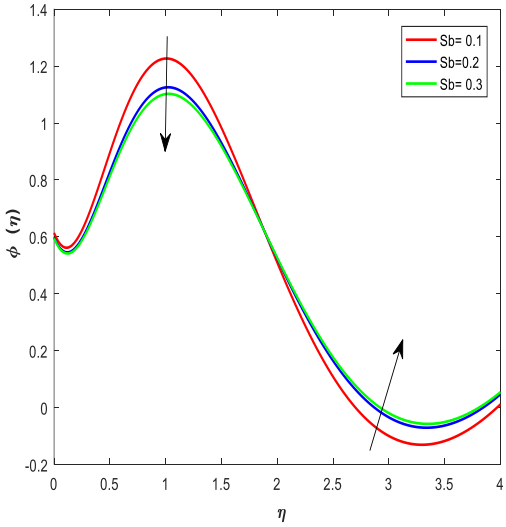

Result 9 (c)

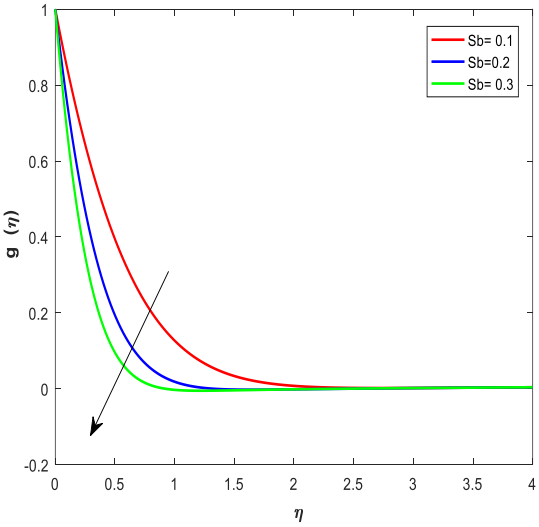

Result 9(d)

Graphical results 10(a)-10(d) represents the impacts of thermal radiation on temperature, the concentration of nanoparticle, and the density of motile microorganisms' profiles

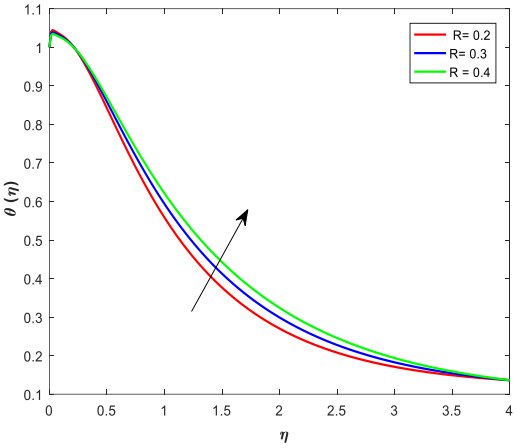

Results 10 (a)

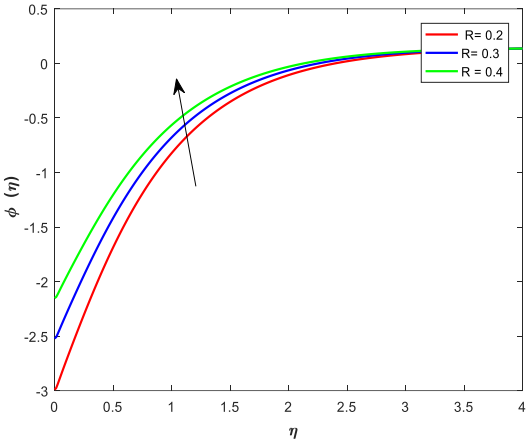

Result 10 (b)

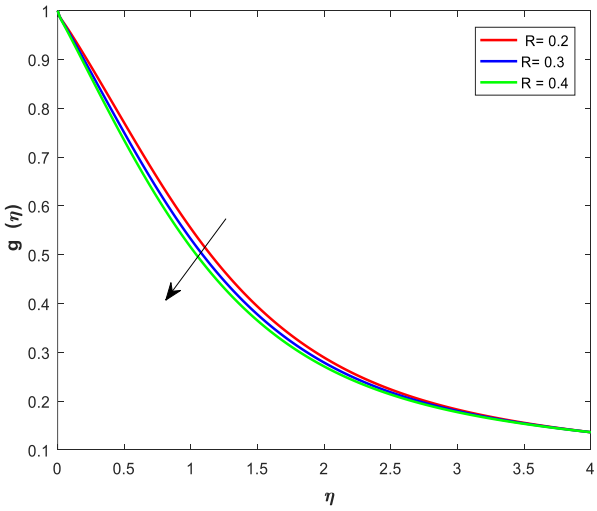

Result in 10 (c)

Graphical results 11(a)-11(c) represents the impacts of Eckert number on temperature, the concentration of nanoparticle, and the density of motile microorganisms' profiles

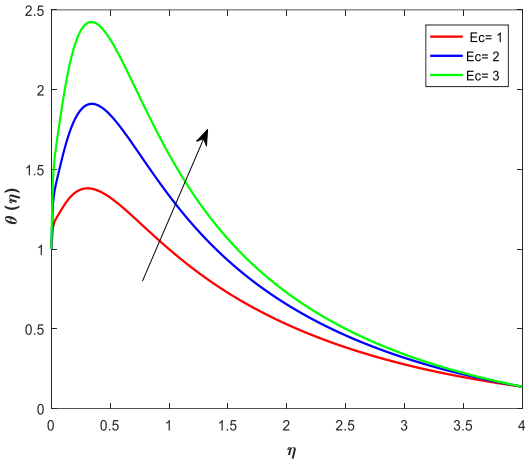

Result 11(a)

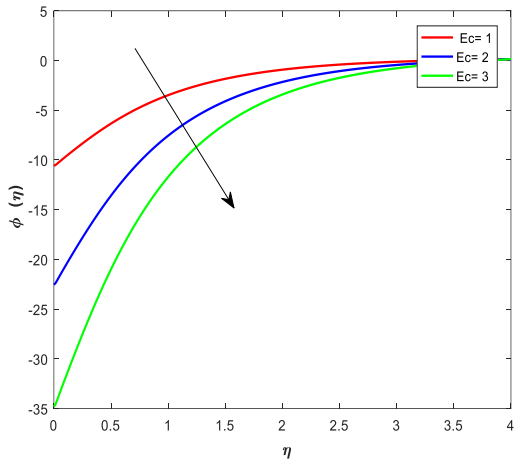

Result 11(b)

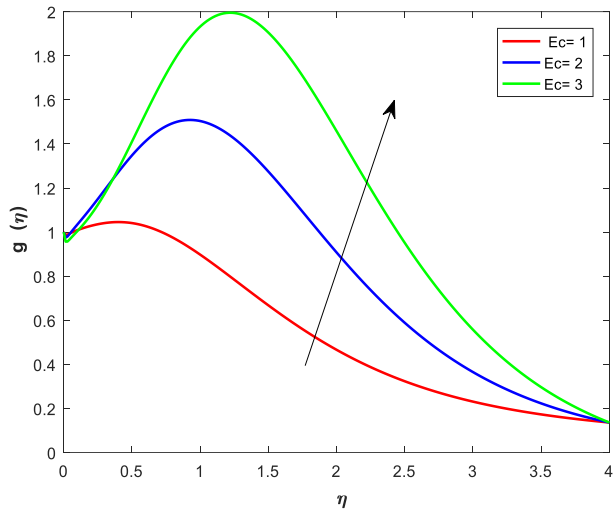

Result 11(c)

Graphical results 12(a)-12(c) represents the impacts of heat generation parameter on temperature, the concentration of nanoparticle, and the density of motile microorganisms' profiles

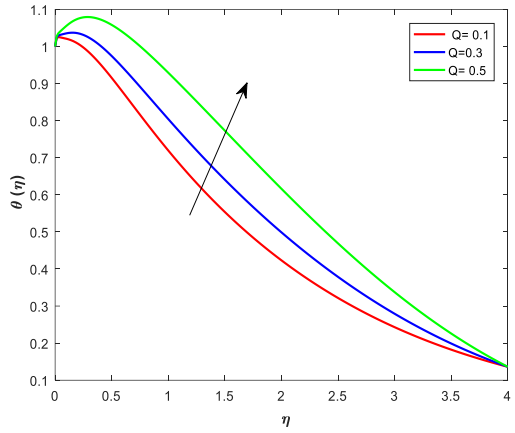

Result 12 (a)

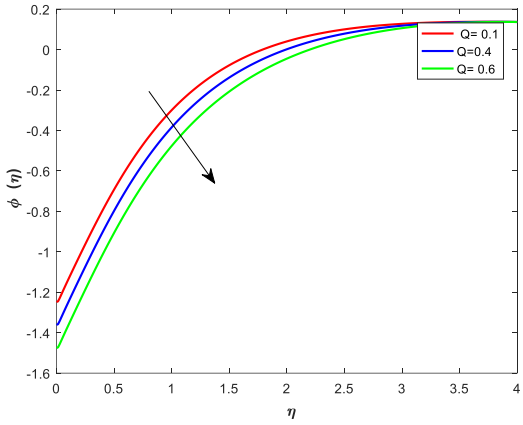

Result 12(b)

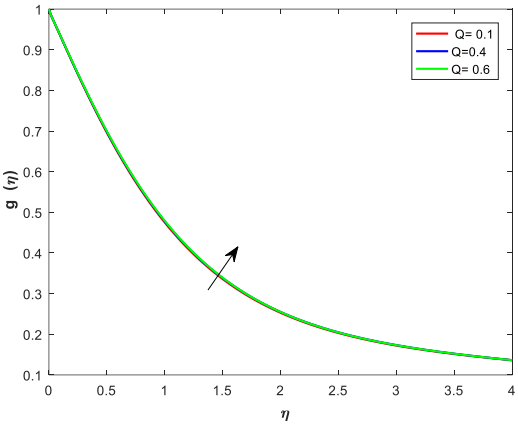

Result in 12 (c)

Conclusions:

The innovative investigation on the bioconvection of heat and mass transfer flow of Walter's B fluid model of nanoliquid interacting with microbes through horizontal porous media is disclosed in this work. In many areas of research and biotechnology, bioconvection flows of microorganisms and nanoparticles are enormously advantageous. The flow model equation system is first numerically simplified by similarity transformations, and then it is solved by the finite difference implicit approach called the Keller Box method.

According to the findings of this investigation, the use of nanoparticles and gyrotactic microorganisms causes the flow to become consistent and stable. The following are the main findings of this analysis.

i) The bioconvection Schmidt number and the motile microbe's parameter increase, which increases the rate at which microorganisms diffuse. But due to an upsurge in bioconvection parameters, a declining trend in the density profiles of motile bacteria is seen.

ii) The heat transfer rate on the surface of the sheet tends to be slowed down by viscous dissipation, which raises the temperature, and density of microorganism's profiles.

iii) When viscous dissipation is absent, the porosity parameter has little effect on the density of motile microorganisms, but when it is present, it significantly affects the density.

References:

[1] U. S. Mahabaleshwar, I. E. Sarris, and G. Lorenzini, "Effect of radiation and Navier slip boundary of Walters' liquid B flow over a stretching sheet in a porous media," *International Journal of Heat and Mass Transfer*, vol. 127, pp. 1327–1337, Dec. 2018, doi: 10.1016/j.ijheatmasstransfer.2018.02.084.

[2] B. J. Akinbo and B. I. Olajuwon, "Impact of radiation and chemical reaction on stagnation-point flow of Hydromagnetic Walters' B fluid with Newtonian heating," *International Communications in Heat and Mass Transfer*, vol. 121, p. 105115, Feb. 2021, doi: 10.1016/j.icheatmasstransfer.2021.105115.

[3] Y.-M. Chu *et al.*, "Thermophoresis particle deposition analysis for nonlinear thermally developed flow of Magneto-Walter's B nanofluid with buoyancy forces," *Alexandria Engineering Journal*, vol. 60, no. 1, pp. 1851–1860, Feb. 2021, doi: 10.1016/j.aej.2020.11.033.

[4] K. V. B. Rajakumar, T. Govinda Rao, M. Umasankara Reddy, and K. S. Balamurugan, "Influence of Dufour and thermal radiation on unsteady MHD Walter's liquid model-B flow past an impulsively started infinite vertical plate embedded in a porous medium with chemical reaction, Hall and ion slip current," *SN Applied Sciences*, vol. 2, no. 4, p. 742, 2020.

[5] M. Sajid, T. Javed, Z. Abbas, and N. Ali, "Stagnation-point flow of a viscoelastic fluid over a lubricated surface," *International Journal of Nonlinear Sciences and Numerical Simulation*, vol. 14, no. 5, pp. 285–290, 2013.

[6] S. A. Madani Tonekaboni, R. Abkar, and R. Khoeilar, "On the study of viscoelastic Walters' B fluid in boundary layer flows," *Mathematical Problems in Engineering*, vol. 2012, 2012.

[7] O. Prakash, D. Kumar, and Y. K. Dwivedi, "Heat transfer in MHD flow of dusty viscoelastic (Walters' liquid model-B) stratified fluid in porous medium under variable viscosity," *Pramana*, vol. 79, no. 6, pp. 1457–1470, 2012.

[8] J. K. Singh, N. Joshi, and P. Rohidas, "Unsteady MHD natural convective flow of a rotating Walters'-B fluid over an oscillating plate with fluctuating wall temperature and concentration," *Journal of Mechanics*, vol. 34, no. 4, pp. 519–532, 2018.

[9] R. Mahat, M. Saqib, I. Khan, S. Shafie, and N. A. M. Noor, "Thermal radiation effect on Viscoelastic Walters'-B nanofluid flow through a circular cylinder in convective and constant heat flux," *Case Studies in Thermal Engineering*, vol. 39, p. 102394, 2022.

[10] M. Ghani, "FREE CONVECTION FLOW OVER A HORIZONTAL POROUS FLAT PLATE WITH THE EFFECT OF MAGNETOHYDRODYNAMICS," *Journal of Fundamental Mathematics and Applications (JFMA)*, vol. 4, no. 2, pp. 139–146, 2021.

[11] H. Xu and I. Pop, "Fully developed mixed convection flow in a horizontal channel filled by a nanofluid containing both nanoparticles and gyrotactic microorganisms," *European Journal of Mechanics-B/Fluids*, vol. 46, pp. 37–45, 2014.

[12] M. I. Khan, F. Alzahrani, and A. Hobiny, "Heat transport and nonlinear mixed convective nanomaterial slip flow of Walter-B fluid containing gyrotactic microorganisms," *Alexandria Engineering Journal*, vol. 59, no. 3, pp. 1761–1769, 2020.

[13] Y.-M. Chu, M. ur Rahman, M. I. Khan, S. Kadry, W. U. Rehman, and Z. Abdelmalek, "Heat transport and bio-convective nanomaterial flow of Walter's-B fluid containing gyrotactic microorganisms," *Ain Shams Engineering Journal*, vol. 12, no. 3, pp. 3071–3079, 2021.

[14] R. Naz, S. Tariq, and H. Alsulami, "Inquiry of entropy generation in stratified Walters' nanofluid with swimming gyrotactic microorganisms, Alexandria Eng," *J*, vol. 59, pp. 247–261, 2020.

[15] S. U. Khan, H. Waqas, T. Muhammad, M. Imran, and S. Aly, "Simultaneous effects of bioconvection and velocity slip in three-dimensional flow of Eyring-Powell nanofluid with Arrhenius activation energy and binary chemical reaction," *International Communications in Heat and Mass Transfer*, vol. 117, p. 104738, 2020.

[16] T. Hayat, "Inayatullah; Alsaedi, A.; Ahmad, B. Thermo diffusion and diffusion thermo impacts on bioconvection Walter-B nanomaterial involving gyrotactic microorganisms," *Alex. Eng. J*, vol. 60, pp. 5537–5545, 2021.

[17] F. Shahzad *et al.*, "Galerkin finite element analysis for magnetized radiative-reactive Walters-B nanofluid with motile microorganisms on a Riga plate," *Scientific Reports*, vol. 12, no. 1, p. 18096, 2022.

[18] H. A. Nabwey, S. M. M. EL-Kabeir, A. M. Rashad, and M. M. M. Abdou, "Gyrotactic microorganisms mixed convection flow of nanofluid over a vertically surfaced saturated porous media," *Alexandria Engineering Journal*, vol. 61, no. 3, pp. 1804–1822, Mar. 2022, doi: 10.1016/j.aej.2021.06.080.

[19] S. Ahmad, J. Younis, K. Ali, M. Rizwan, M. Ashraf, and M. A. Abd El Salam, "Impact of swimming gyrotactic microorganisms and viscous dissipation on nanoparticles flow through a permeable medium: a numerical assessment," *Journal of Nanomaterials*, vol. 2022, pp. 1–11, 2022.

[20] A. S. Oke *et al.*, "Exploration of the effects of Coriolis force and thermal radiation on water-based hybrid nanofluid flow over an exponentially stretching plate," *Sci Rep*, vol. 12, no. 1, Art. no. 1, Dec. 2022, doi: 10.1038/s41598-022-21799-9.

[21] Q.-H. Shi *et al.*, "Numerical study of bio-convection flow of magneto-cross nanofluid containing gyrotactic microorganisms with activation energy," *Sci Rep*, vol. 11, no. 1, Art. no. 1, Aug. 2021, doi: 10.1038/s41598-021-95587-2.

[22] R. J. Punith Gowda, R. Naveen Kumar, A. M. Jyothi, B. C. Prasannakumara, and I. E. Sarris, "Impact of Binary Chemical Reaction and Activation Energy on Heat and Mass Transfer of Marangoni Driven Boundary Layer Flow of a Non-Newtonian Nanofluid," *Processes*, vol. 9, no. 4, Art. no. 4, Apr. 2021, doi: 10.3390/pr9040702.

[23] R. N. Kumar, P. B.c, and R. J. P. Gowda, "Impact of diffusion-thermo and thermal-diffusion on the flow of Walters-B fluid over a sheet saturated in a porous medium using local thermal non-equilibrium condition," *STRPM*, doi: 10.1615/SpecialTopicsRevPorousMedia.2023045844.

[24] A. V. Kuznetsov and D. A. Nield, "The Cheng–Minkowycz problem for natural convective boundary layer flow in a porous medium saturated by a nanofluid: a revised model," *International Journal of Heat and Mass Transfer*, vol. 65, pp. 682–685, 2013.

[25] X. Wen, D. B. Ingham, and B. Widodo, "The free surface fluid flow over a step of an arbitrary shape in a channel," *Engineering Analysis with Boundary Elements*, vol. 19, no. 4, pp. 299–308, Jun. 1997, doi: 10.1016/S0955-7997(97)00038-6.

Nomenclature:

M	Magnetic field parameter
P	Porous media
Pr	Prandtl number
R	Thermal radiation number
Nb	Brownian motion parameter
Nt	Thermophoresis parameter
Ec	Eckert number
Q	Heat transfer coefficient
Sc	Schmidt number
A	Chemical reaction parameter
Sb	bioconvection number
Pe	Peclet number
u, v	Velocity components
x, y	axis coordinates